Review

Zhenjia Huang, Gary Chi-Pong Tsui*, Yu Deng, and Chak-Yin Tang

Two-photon polymerization nanolithography technology for fabrication of stimulus-responsive micro/nano-structures for biomedical applications

https://doi.org/10.1515/ntrev-2020-0073
received August 24, 2020; accepted September 16, 2020

Abstract: Micro/nano-fabrication technology via two-photon polymerization (TPP) nanolithography is a powerful and useful manufacturing tool that is capable of generating two dimensional (2D) to three dimensional (3D) arbitrary micro/nano-structures of various materials with a high spatial resolution. This technology has received tremendous interest in cell and tissue engineering and medical microdevices because of its remarkable fabrication capability for sophisticated structures from macro- to nano-scale, which are difficult to be achieved by traditional methods with limited microarchitecture controllability. To fabricate precisely designed 3D micro/nano-structures for biomedical applications via TPP nanolithography, the use of photoinitiators (PIs) and photoresists needs to be considered comprehensively and systematically. In this review, widely used commercially available PIs are first discussed, followed by elucidating synthesis strategies of water-soluble initiators for biomedical applications. In addition to the conventional photoresists, the distinctive properties of customized stimulus-responsive photoresists are discussed. Finally, current limitations and challenges in the material and fabrication aspects and an outlook for future prospects of TPP for biomedical applications based on different biocompatible photosensitive composites are discussed comprehensively. In all, this review provides a basic understanding of TPP technology and important roles of PIs and photoresists for fabricating high-precision stimulus-responsive micro/nano-structures for a wide range of biomedical applications.

Keywords: micro/nano-fabrication, two-photon polymerization, stimulus-responsive structure, biomedical applications

1 Introduction

Well-defined three-dimensional (3D) structures with micro- or nano-features are of great interest for diverse bioapplications including cell engineering [1], tissue engineering [2,3], biorobots [4]. microfluidic systems [5] and drug delivery [6,7]. In order to fabricate desirable hierarchical 3D architectures, various kinds of manufacturing techniques, such as selective laser sintering (SLS) [8], stereolithography (STL) [8,9] and electrospinning [10,11], have been developed. Although many two-dimensional (2D) nanopatterns and simple 3D microstructures can be manufactured by the aforesaid technologies, precise control of the submicron to nanometer-sized features is still difficult to be achieved. Direct laser writing (DLW) via two-photon polymerization (TPP), as a novel emerging prototyping technique, has attracted enormous research attention in the past few decades because of its high spatial resolution and ultraprecision in photopolymerization not only on the microscopic scale but also on the nanoscale [12]. Unlike conventional single-photon polymerization induced by an ultraviolet (UV) laser, a photoinitiator (PI) molecule in a polymerizable resist consisting of monomers or oligomers absorbs two photons simultaneously to initiate polymerization in a highly localized region around the center of the focused

* **Corresponding author: Gary Chi-Pong Tsui,** State Key Laboratory of Ultra-precision Machining Technology, Department of Industrial and Systems Engineering, The Hong Kong Polytechnic University, Hung Hom, Kowloon, Hong Kong, China; Advanced Manufacturing Technology Research Centre, Department of Industrial and Systems Engineering, The Hong Kong Polytechnic University, Hung Hom, Kowloon, Hong Kong, China, tel: +852 3400 3254, fax: +852 2362 5267, e-mail: gary.c.p.tsui@polyu.edu.hk
Zhenjia Huang: State Key Laboratory of Ultra-precision Machining Technology, Department of Industrial and Systems Engineering, The Hong Kong Polytechnic University, Hung Hom, Kowloon, Hong Kong, China; Advanced Manufacturing Technology Research Centre, Department of Industrial and Systems Engineering, The Hong Kong Polytechnic University, Hung Hom, Kowloon, Hong Kong, China
Yu Deng: School of Electromechanical Engineering, Guangdong University of Technology, Guangzhou, China
Chak-Yin Tang: Advanced Manufacturing Technology Research Centre, Department of Industrial and Systems Engineering, The Hong Kong Polytechnic University, Hung Hom, Kowloon, Hong Kong, China

beam via nonlinear absorption. A solid volume pixel, known as a voxel in micro/nano-fabrication, is then created [13]. Based on this voxel-by-voxel approach, sophisticated design features can be realized in specific areas of structures by a tightly focused laser beam without the need to use photomasks. The scanning path of the laser beam is commonly moved along a 2D scanning path, while layer-by-layer scanning along the vertical axis enables the printing process of 3D architectures. The polymerization rate is proportional to the square of the equipment laser intensity. Therefore, sub-100 nm resolution can be achieved using a high numerical aperture (NA) objective lens with the advent of femtosecond and picosecond laser pulse [14]. Other polymerization mechanisms triggered by nonlinear absorption of photons such as three-photon absorption [15] are also possible.

To exploit the potential applications of TPP, various optically transparent photosensitive materials have been engineered, leading to the fabrication of 3D microstructures with remarkable functions due to the presence of unique micro/nano-structure features which are difficult to be produced by conventional methods. Most of the typical photopolymerizable materials for TPP nanolithography resemble those utilized for traditional UV lithography. The difference of absorption in photons distinguishes the spatial resolution of structures. The most popular materials developed for single-photon STL decades ago are acrylate-based and epoxy-based resins which are photosensitized by an excimer laser at 308 nm wavelength or Hg-lamp at 365 nm [16–18] and can also be applied in the TPP-DLW nanolithography system. A large diversity of micro-objects, including micro/nano-electromechanical systems (MEMS/NEMS) [19–21], micro/nano-photonics [22], biomimetic interfaces and architectures [23,24], have been fabricated by TPP based on these materials.

In particular, when biocompatible and non-cytotoxic photoresists (hydrogel, photo-crosslinkable proteins, commercial IP-series photoresists and other hybrid materials) and water-soluble PIs are used, TPP is capable of generating 3D matrices featured by outstanding stability and excellent biocompatibility with natural tissue environments [25–28]. In addition, TPP uses a light source lying in a near-infrared (NIR) region, which makes it possible to conduct the photopolymerization in photoresist loaded with living cells [29]. The native microenvironments where cells reside, namely, extracellular matrix (ECM), possess complex networks from the macroscale to nanoscale which can regulate cell behavior and tissue differentiation [30–32]. Although some scaffolds with micro/nano-features can be manufactured by some approaches, such as solvent casting and particle leaching [33], electrospinning [34] and emulsion freeze-drying [35], micro/nano-features generated by the aforementioned technologies cannot be controlled in terms of size and shape for mimicking the natural microenvironments. Therefore, how structural features affect the interaction between cells and scaffolds have been hindered by limitations of the conventional methods. Instead, well-organized scaffolds fabricated by TPP can mimic the natural microenvironment of human tissue with respect to multi-scale structures. They serve as a versatile platform to promote the regulation of cell behavior, including cell attachment, proliferation, differentiation and cell-to-cell interaction [36]. Development of novel drug transportation and release systems has also been enabled with the coming of precise structural design by computer-aided CAD software and the minimization of microdevices by TPP [37]. Desirable temporal and spatial distribution of drugs *in vitro* and *in vivo* can be achieved by the design of a special drug-loaded scaffold. Moreover, microneedle enhancing drug delivery is of advantage in solving many issued problems associated with intravenous drug administration, including pain to the patients resulting from the traditional metal needles, trauma in the injection site and long-term sustainable release of the medicine [38].

This paper aims to provide an up-to-date and comprehensive account of the TPP research field, with emphasis on conventional and stimulus-responsive photosensitive materials and their biomedical applications. As PIs and photoresists play crucial roles in fabricating stimulus-responsive micro/nano-structures via TPP technology such as spatial resolution of the structures and their manufacturing time, currently widely used PIs and different photoresists are summarized systematically in terms of their properties and two-photon absorption capability. Meanwhile, a selection of distinctive previous studies that can potentially project the future trends of TPP in the biomedical field is discussed with featured versatile applications of 3D nano/micro-constructs based on the aforementioned materials. Finally, current limitations and challenges in the material and fabrication aspects as well as the outlook on future prospects of TPP for biomedical applications are described.

2 TPP PIs for biomedical applications

Unlike the single photon absorption process, to trigger the TPA process, one atom or molecule must simultaneously absorb two photons to arrive at an excited state

from the ground stage to induce the transition, which can be realized by an ultrafast laser beam with a high intensity of the pulse peak. After immediate excitation, the TPA process occurs within a small focal volume in the photopolymerizable materials to ensure a high resolution. Then chemical polymerization between the initiators and monomers will occur [39,40]. Based on this process, photosensitive monomers with active moieties can react with reactive species (e.g., free radicals or cations) generated by photosensitive molecules to form 3D micro/nano-structures. A typical photoresist system contains (1) one or more PIs or photosensitizer(s) with absorption near the two-photon excitation wavelength; (2) transparent photocurable polymeric monomers with functional groups in the NIR wavelength. In most research, some other materials (cross-linkers, nanoparticles, etc.) are added into the aforementioned photoresists to achieve special properties. During this modification procedure, organic or inorganic solvents are usually used to dissolve and dilute the above individual components for liquid-based photoresists with controlled viscosity.

The overall photopolymerization procedures can be divided into the following three steps: initiation, propagation and termination [41]. For the initiation step, it is critically significant to choose highly active PIs so that full potential of the TPP technique can be realized. PIs can affect the mechanism of chemical polymerization, as well as the polymerization reaction rate and the final properties of the formed polymer including its hardness and viscosity [42]. Molecules with a large TPA cross section (δ_{TPA}) and high-initiating efficiency are in tremendous demand [43]. δ_{TPA} is widely used in the evaluation of TPA performance of molecules, and it is measured in Goeppert–Mayer (GM) units (1GM = 10^{-15} cm^4 per photon molecule). Currently, a variety of molecules with enhanced δ_{TPA} have been designed and synthesized. The structure–property relationship between the molecule structure and δ_{TPA} was summarized by Perry et al. [44]. The intermolecular charge transfer efficiency (ITCE) has been demonstrated to be a key parameter in evaluating the δ_{TPA} performance of one molecule. Several research studies have been reported to increase the δ_{TPA}, by extending the length of the π-conjugated chains, introducing strong electronic acceptor and donor moieties and increasing the molecular coplanarity [45–47].

Thereby, PIs with a high TPA cross section and high initiation efficiency undoubtedly play an important role in the TPP micro/nano-fabrication process. The size of TPA-triggered polymerized voxels is a significant feature for fabricating micro/nano-structures because it determines the capacity of achieving a sub-diffraction-limited structural resolution. Moreover, the chemical polymerization can be carried out at a low excitation laser power (less than 180 mW) and short exposure time, which further brings about a fast scanning speed and desired printing quality. The selection of an appropriate PI is essential for achieving a desirable initiation rate and structural properties. With the low photon energy of NIR light used in TPP, some polymerization processes can be manipulated in the presence of cells or whole organisms [48,49]. When being applied in biomedical fields, PIs are required to be noncytotoxic to the surrounding cells or tissues. In most biocompatible photoresist systems such as hydrogel-based natural or artificial materials, they also need to be soluble and thermally stable in the monomer aqueous microenvironments [42]. Currently, a lot of PIs, such as rose bengal, methylene blue, lithium phenyl-2,4, 6-trimethyibenzoylphosphinate (LAP) and Irgacure 369, are available commercially and commonly used for fabricating micro/nano-structures for biomedical applications [26,36,50–52]. In Table 1, PIs for the TPP fabrication are summarized along with their water solubility, δ_{TPA}, and biomedical applications as reported in some studies.

To improve the water solubility of PIs in aqueous solutions, non-ionic surfactants have been added to conventional hydrophobic PIs. Jhaveri et al. [54] undertook the microfabrication of hydrogels via TPP in aqueous solution by adding a surfactant Pluronic F127 into a commercially available initiator Irgacure 651. Although this method is effective, a high surfactant concentration is needed to achieve initiation efficiency. Excessive surfactants may further reduce the biocompatibility of the final developed structures or even bring about cytotoxicity, which is unacceptable to the subsequent biomedical applications. Some other hydrophilic PIs and xanthene dyes, such as Irgacure 2959 [55], rose bengal and methylene blue [56], have gained a lot of research attention for TPP. Irgacure 2959, one of the first commercially available PIs, has been widely used in the fabrication of 3D hydrogel scaffolds because of its biocompatibility and low cytotoxicity, but it is only processable for TPP at a wavelength of 515 nm, which may cause the denaturation of proteins [55,57]. Moreover, its low water solubility below 2% leads to unsatisfactory polymerization efficiency. Rose bengal, methylene blue and Eosin-Y have very low δ_{TPA} values (only 10GM at 800 nm), which require long exposure time (300–400 μs) and high laser intensity, resulting in a time-intensive process.

Table 1: Typical PIs for TPP and their properties and applications

PIs	Solubility in water (mg/mL)	δ_{TPA}	Photoresist and application	Reference
Rose bengal	100	10	Gelatin methacrylamide and BSA, 3D polymer–protein hybrid scaffolds	[26]
Eosin Y	400	10	Two-photon excited photodynamic therapy	[50]
LAP	29	Not known	PEGDA, suspended structures (≤1 μm) with tunable Poisson's ratios for fibroblast cell behavior study	[51]
Irgacure 369	0	7	PEGDA, 3D scaffolds for optical interrogation and neurite guidance of human iPSC-derived neuronal networks	[52]
Irgacure 2959	10	Not known	Methacrylated chitosan, 3D ring-like micro-scaffold for human pulmonary microvascular endothelial cells culture	[36]
WSPI	High	120	PEGDA, 3D woodpile scaffolds in living organisms	[48]
P2CK	High	176	PEGDA, 3D woodpile structures for tissue engineering	[53]

In order to synthesize efficient water-soluble PIs, the most effective method is to introduce water-borne functional groups such as quaternary ammonium salts or different sodium carboxylic salts into the well-investigated chromophore core structures which have high TPA activity. Among the synthesized PIs, a large covalent structure like alkyl chains of different lengths and benzylidene are usually needed to avoid shifting the electronic structure of the TPA chromophore, as shown in Figure 1. For example, when quaternary ammonium cations are introduced, the synthesized water-soluble WSPI initiator (1,4-bis(4-(*N*,*N*-bis(6-(*N*,*N*,*N*-trimethylammonium)hexyl)amino)-styryl)-2,5-dimethoxybenzene tetraiodide) shows a high δ_{TPA} value of 120 GM. Torgersen et al. [48] first fabricated 3D woodpile scaffolds with high water content using poly(ethylene glycol)diacrylate (PEGDA) and WSPI in the presence of living organisms, which laid the foundation for *in vivo* microfabrication via TPP for tissue engineering applications. WSPI was also used in a thiol–vinyl copolymer system to fabricate 3D protein hydrogels [58]. Sodium carboxylic groups were also incorporated at the terminal alkyl chains to generate a series of PIs for direct encapsulation of living cells by TPP under aqueous conditions, such as P2CK [53] G2CK [59], BSEA [60] and E2CK [61].

Recently, a newly emerging effective method to increase the solubility of hydrophobic PIs in aqueous solution was completed by a host–guest chemical interaction. Some macrocyclic host molecules, such as cyclodextrins (CDs) and cucurbit[*n*]urils (CB[*n*]s), can encapsulate hydrophobic PIs as guests to form host–guest inclusion complexes [62–64]. Due to their supramolecular structures, CDs and CB[*n*]s both had one hydrophobic cavity and a hydrophilic outer surface contributed by the hydroxyl and carbonyl functional groups, respectively. The driving force for the generation of the host–guest structure between the macrocyclic host molecules and guest molecules mainly resulted from the following two factors: (1) the hydrophobic effect to release the high-energy water stuck in the host cavities; (2) electrostatic attraction between the electron-rich surface of the host molecules and the electron-deficient parts of the guest molecules [65–68]. Therefore, many researchers have synthesized different host–guest complexes with different types of CDs and CB[7]s, one example with good aqueous solubility and low cytotoxicity in the CB[*n*]s family. Duan's group [69] has done a lot of work and studied their δ_{TPA} properties. For example, when hydrophobic 2,7-bis(2-(4-pentaneoxyphenyl)-vinyl) anthraquinone was assembled with

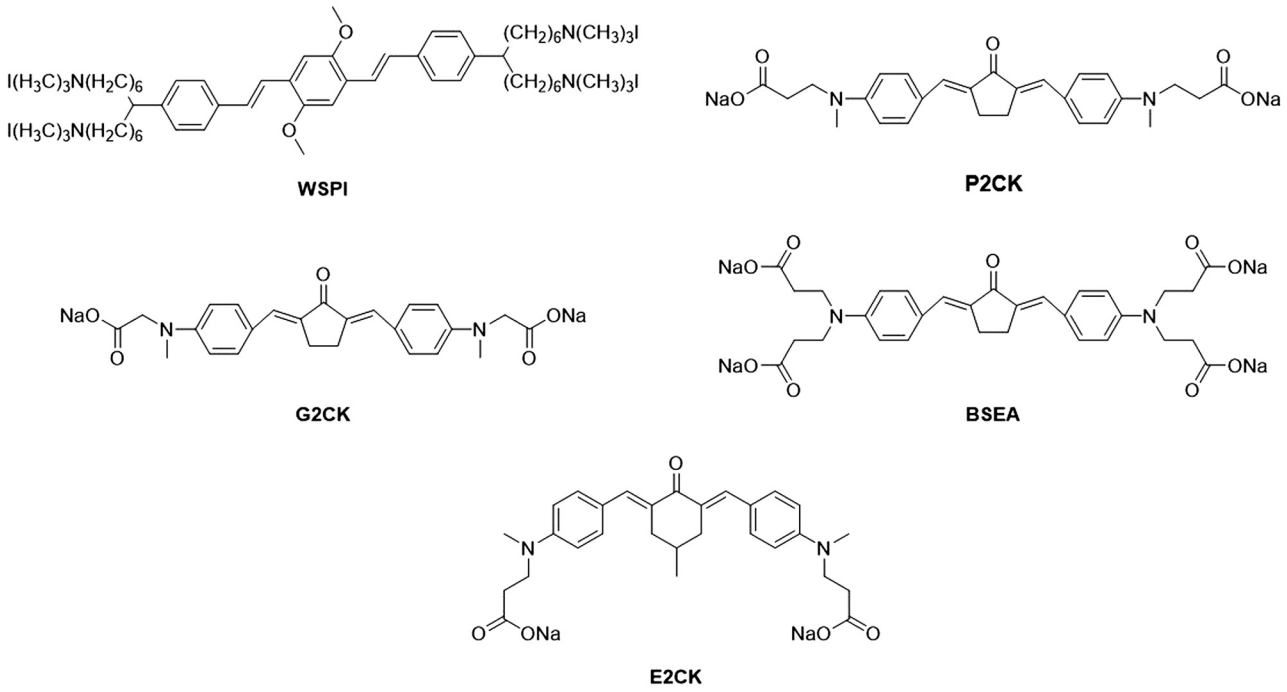

Figure 1: Molecular structures of water-soluble PIs for biomedical application.

2-hydroxypropyl-β-CDs, this water soluble TPP initiators had a δ_{TPA} value of around 200GM at a 780 nm wavelength. At the same time, the TPP threshold energy in water was 8.6 mW when using PEGDA with this PI [70]. 3,6-Bis[2-(1-methyl-pyridinium) vinyl]-9-pentyl-carbazole diiodide (BMVPC) exhibited a high δ_{TPA} value attributed to its A–π–D–π–A structure. However, it has limited biomedical application via the TPP technology due to its low solubility and initiating effect in spite of its good biocompatibility and hypotoxicity [71]. By incorporating BMVPC with CB[7]s, Zheng et al. [72] created a host–guest complex BMVPC-CB[7]s with a very high δ_{TPA} value up to 2,999GM at a wavelength of 800 nm. When being applied in PEGDA photoresist, a high spatial resolution of 180 nm was achieved by using a relatively low laser threshold of 4.5 mW.

3 TPP-compatible photoresists

Most of the materials for TPP are similar to those used in the conventional UV lithography method, in which the materials are usually in the form of viscous liquid, amorphous solid or gel. Negative- and positive-tone photoresists are the two typical photosensitive materials. For negative-tone photoresists, two-photon exposure leads to a cured 3D structure on a substrate directly via crosslinking of polymer chains, leaving the unpolymerized photoresists to be washed out by a developing solvent. In contrast, for the positive-tone photoresists, they are first solidified by an UV laser or heat. Then the NIR laser beam exposure results in the breakup of the photoresist polymer chains through photoacid degradation, generating shorter units which can be dissolved and washed away in the development process [73]. Negative-type photoresists, including the commercially available epoxy-based photoresists (e.g., SU-8; MicroChem) [74], acrylate-based photoresists (e.g., IP-Series resists; Nanoscribe GmbH) [75] and the hybrid sol–gel ORMOCER (Microresist Technologies) [76] with low shrinkage and superior chemical stability, are the most widely used. Positive-tone photoresists are efficient in fabricating hollow structures with only a small fraction removed from the whole material in the original workpiece [77]. Moreover, such hollow constructs can serve as good master templates/molds for indirect manufacturing. Although it is convenient to carry out 3D scaffold fabrication using the aforementioned photoresists, they are proprietary materials and cannot be easily modified or incorporated with other components for customized functionalities such as tunable modulus or single- or multi-stimulus-responsive behavior. This has limited their use for bioapplications via TPP, especially fabrication of dynamic cell or tissue engineering scaffolds, microactuators in medical

Tablee 2: Types of microstructures fabricated from various IP-series photoresists and their application

Photoresist systems	Bioapplication	Structures	Performance	Reference
IP-L 780	Drug screening	3D cell cage assembly	Enable multilayer stacking of different types of cells	[91]
	Cell engineering	3D architectures with different Young's modulus and stiffness gradients	Pave a unique way to study single tumor cell dynamics in surrounding environment with different modulus	[92]
IP-Dip	Cell engineering	3D woodpile scaffold	Reveal the mechanisms of cell proliferation and colonization	[93]
IP-S	Regenerative therapy	3D porous scaffolds	Support induced pluripotent stem cell (iPSC) adhesion, proliferation and differentiation	[94]
	Drug delivery	Microneedle arrays	Achieve more effective multicomponent cutaneous vaccination using undercut microneedle arrays	[37]
IP-G 780 with Ni/Cr layers	Microswimmers	Helical structures	Possess high sensitivities to both the magnetic propulsions and the fluorescence	[95]
IP-Visio	Microfluidics	3D microfluidic channel	Tailor gas dynamic virtual nozzles function to achieve jet diameters below 100 nm for single-particle imaging	[96]

devices or microfluidics. Table 2 provides some typical bioapplications based on these commercially available materials.

To facilitate the biomedical applications of TPP, lots of stimulus-responsive photoresist systems have been developed to prepare 3D structures. Functional groups in the monomers or nanoparticle dopants can both make the scaffolds respond to external stimuli. Because of the similarity of mechanical and diffusivity properties as compared with those of ECM, a wide variety of hydrogel-based photoresists made of natural biopolymers or proteins and synthetic polymers have been used to fabricate stimulus-responsive microstructures via TPP for biomedical applications. The use of monomers or oligomers with different functional groups resulted in micro/nano-structures exhibiting dynamic properties such as actuation [78–80], shape-shifting capabilities [81] under different stimuli such as pH, solvent, light and temperature. Most significantly, the mechanical properties of hydrogels could also be tuned by adjusting its high water content (≥10%) in a 3D porous polymeric network except the crosslinking degree, which supports cell attachment and further growth [82]. However, only a few of them are commercially available at present.

Liquid crystalline elastomers (LCEs), as smart artificial materials that are capable of providing feedback to different external stimuli, have recently drawn extensive scientific attention in novel biomimetic functional micro/nano-structured systems [83–85]. They possess the advantages of high elasticity and contractility with an ability to undergo completely reversible shape-change behavior triggered by stimuli such as heat, humidity, light and electrical and magnetic fields [86]. They can be manufactured in various 2.5D or 3D forms via TPP, such as micro/nano-patterned substrates, porous scaffolds and well-designed microrobots. For some soft contractile tissues of mammals, cellular alignment in the same direction, which is notable in cardiac and muscular tissues [87], plays a key role in contraction force generation. Based on the liquid crystalline to isotropic phase transition, the actuation force generated by LCE sheets or scaffolds can be used to dynamically train cells for acquiring desirable alignment and promoting elongation, which has become one of the promising methods to engineer such tissues for repair and regenerative therapies [88,89]. Moreover, well-designed microrobots loaded with drugs can be transported to a target location in the human body for preventing and treating the spread of cancer. Although research on LCEs is a well-established field, biomedical application of micro/nano-textured systems fabricated

Table 3: Types of stimulus-responsive photoresists and their microstructures fabricated by TPP for biomedical applications

Stimulus	Photoresists and PIs	Bioapplication	Microstructures	Reference
pH	BSA and rose bengal	Actuators	Dual-pillar cross-shaped microstructures and microtrap	[81]
	BSA and rose bengal	Microfluidics, cell micropatterning	Geometrical shape-shifting microstructures with sandwich-based design	[97]
	BSA and rose bengal	Microdevices, tissue engineering	3D microsieves with changing pore size	[98]
	PEGDAs, CEA and Irgacure 819	Biosensing	Micropyramid and microdome with different swelling action	[99]
Light	LC monomers, LC crosslinker, azo dyes and Irgacure 369	Biorobots	A cuboid body and conical legs	[100]
	LCE, AuNRs and Irgacure 369	Microactuators or robotic devices	Woodpile structures, microclamp structures with gripping behavior.	[101]
	PNIPAAm, PEGDA, Fe_3O_4 nanoparticles and Benzil	Microactuators	Microstructures with deformable two microcantilevers and micropedestal	[78]
Electromagnetic field	SU-8, Fe_3O_4 nanoparticles	Drug delivery, single-cell manipulation	3D cube and helical microswimmers	[102]
	SU-8, Ni/Ti bilayer	3D cell transportation and drug delivery	3D porous microniches	[103]
	Acrylamide, PEGDA, Fe_3O_4 NPs and benzyl	Sensors and actuators	Largely bendable micronail	[104]

by TPP based on these materials is a relatively new field. In addition, most sheets or scaffolds are generated by traditional manufacturing technologies which require templates or masks. Some complex 3D structures with micro/nano-patterns are difficult to be fabricated by these technologies. Herein, in the following sections, the development of TPP compatible photoresists, focusing on the commercially ready-to-use types and the smart types with stimulus-responsiveness based on the stimulus (pH, light and magnetic field), is reviewed and summarized in Table 3.

3.1 Ready-to-use commercially available photoresists for TPP

Proprietary IP-photoresists from Nanoscribe GmbH are negative types without extra addition of PIs especially developed for TPP DLW via non-linear absorption of femtosecond NIR laser beams. They exhibit extraordinary spatial resolution, high mechanical stability and easy handling for 3D structures in the micro and submicron range. Up to now, the advantageous features of IP-photoresists have been well demonstrated by a wide application range. Among these photoresists, IP-L 780, IP-Dip, IP-S and IP-Q are designed for the DiLL configuration. IP-G 780 is suitable with an oil immersion configuration. IP-L780 resin, IP-Dip and IP-G 780 were reported to achieve submicron features, low shrinkage and high aspect ratios for the fabricated parts, rendering their potential application in biomimetic surfaces. Micro- and mesoscale structures prepared by IP-S generally possess smooth surfaces with a good shape accuracy. Recently, another newly introduced resin IP-Visio, reported to have low fluorescence and non-cytotoxicity, has also become available for life science research and is suitable for use in 3D cell scaffolds, tissue engineering and biomedical devices [90]. Moreover, some post-printing processes, such as atomic layer deposition, chemical vapor deposition or galvanization, can be used to modify 3D structures for additional functions.

3.2 Customized smart materials for TPP

3.2.1 pH-responsive photoresists

pH-sensitive photoresists can undergo dynamic swelling changes that influence their volume and elasticity in

response to the slight altering of the surrounding pH value because they have functional moieties such as carboxylic (–COOH) and amino ($–NH_2$) groups that can respond to a pH change [81,97]. pH-responsive hydrogels are the mostly studied photoresist monomers. The swelling behavior of hydrogels with carboxylic or amino pendant groups depends on the difference of the pK_a values of carboxylic groups or the pK_b values of amino groups relative to environmental pH. A lower or a higher pH value of the surrounding medium than the dissociation constants of the pendant groups could induce the increase of charges in the pendant groups, leading to the electrostatic repulsion between the polymer chains [105].

A representative example of a pH-sensitive hydrogel used in TPP is bovine serum albumin (BSA)-based hydrogel whose globular structure resembles to that of human serum albumin. It is a highly water-soluble monomeric protein containing 583 amino acid residues. Therefore, it is the most widely used protein for the preparation of 3D structures via TPP for cell behavior studies and tissue engineering. At the isoelectric point of pH, BSA proteins are hydrophobic without a net charge, leading to an increase of the aggregation of protein molecules. Less water is absorbed by the polymer network, which results in shrinkage of the protein gel [106]. On the other hand, at the altered pH point, amino acids in the protein chains become ionized due to protonation of their amino functional groups or deprotonation of carboxylic groups. The increasing number of ions in the protein can further facilitate the repulsion of the molecules and the interaction with water via ion–dipole interaction, thereby causing the protein structures to swell [97,98].

BSA proteins have been used to fabricate microstructures with anisotropic and programmable shape deformation ability by means of TPP. Using TPP, a dynamic and reversible BSA-based Venus fly trap was created. When the pH value was changed from 5 to 11, four tips of the structure would bend inward to generate a closed trap [81]. Additionally, by patterning microstructures with low and highly cross-linked changing parts, dynamic circle-to-polygon and polygon-to-circle shape-shifting can be realized by changing the pH [97]. This will potentially enable controllable connectivity and porosity in 3D microfluidics for biosensors.

Other hydrogels can also be used to achieve pH-responsive action by the chemical functionalization of carboxylic-based materials. Among these biocompatible hydrogels, polyethylene glycol-based hydrogels have been the most attractive for bioapplications for many years [107,108]. A number of advantages, including low-protein absorption, *in vivo* safety with negligible inflammatory profile and easy functional modification, have made it become "gold standard" material for cell and tissue engineering. Scarpa et al. [99] first used biomolecule, 2-carboxyethyl acrylate (CEA), to confer high-molecular-weight PEGDA with pH sensitivity. Different microstructures showed different deformation actions under varying pH values. Micropyramids exhibited a large degree of shape change between high and low pH values, while microdomes maintained their shape with only a dimensional change.

pH-responsive biomaterials composed of BSA and other hydrogels have also been investigated. Kaehr and Shear [109] incorporated BSA proteins into poly(methyl methacrylate) (PMMA) for the fabrication of microscopic 3D structures via TPP. The protein microstructures were demonstrated to maintain ligand-binding and catalytic functionality. Therefore, after the TPP fabrication process, electrostatic and hydrophobic interactions that control protein conformation remained intact in the microchamber. By well-defining the spatial gradients of protein in the PMMA hydrogel matrix, the microchamber had distinct capacity for expansion and contraction in response to changes in a chemical environment. Then, for example, this responsive microstructure could trap, incubate and release motile cells such as *Escherichia coli* passively. At the pH 7, the microchamber could capture motile cells and provide a suitable environment for the growth. When the pH value was changed from 7 to 12.2, the hydration level of the protein-based microchamber walls was changed greatly, inducing a temporary compression of the internal microchamber. Trapped cells were then released into the outside aqueous environment.

Although BSA-based pH-responsive photoresists are promising for biomedical applications, there remain some limitations that need to be considered. As the single component BSA lacks mechanical stability, it may be overcome by combining BSA with other hydrogels to form hybrid materials. In future, more types of hybrid photoresists composed of proteins and hydrogels can be considered to be explored for TPP due to their great demand for various biomedical applications.

3.2.2 Light-responsive photoresists

Light, one of the remotely controllable stimuli, has attracted the most research interest for smart materials. In general, light-induced actuation of polymers has two main types: photoisomerization of chromic moieties in a

chain of monomers and the photothermal effect of nanoparticles in heat-responsive polymer matrices [110–112]. The *cis–trans* isomerization photoresponse of azobenzene function groups is commonly used in light-responsive photoresists. Most LCEs contain azobenzene photochromic molecules characterized by –N=N– linkage, which are able to induce the phase transition isothermally [113]. The azobenzene moiety can undergo reversible isomerization between its two geometric isomers under light of appropriate wavelength. The *trans* form of azobenzene has a rod-like shape that can stabilize the liquid crystalline phase, while the *cis* form can disrupt this stable phase order. Therefore, macroscopic deformation of LCEs could be induced by the change of phase order of the azobenzene moieties in LCE chains [114]. Moreover, LCEs are known as smart materials because of the anisotropic properties of the liquid crystals and the elastic behavior of their polymeric networks similar to that of traditional rubber [115,116]. These properties depend on their glass transition temperature (T_g), which is usually below room temperature. When the surrounding environment temperature is below T_g, the mesogens (liquid crystalline phases) in the monomer chains have an anisotropic and elongated conformation. Once the temperature is higher than T_g, the mesogens can become randomly aligned, leading to random coil conformation of chains [117].

A large number of applications have been undertaken for micro/nano-robotics based on the capability of LCEs to transform light into mechanical force. A typical one is the light-fueled microscopic walkers made of an azobenzene-containing LCE body (their own muscle) and four IP-Dip conical rigid legs, as proposed by Zeng and co-workers [100]. Actuated by a 532 nm laser beam at 50 Hz, this tiny LCE walker with a dimension of $60 \times 30 \times 10\,\mu m^3$ could contract along one side, which further triggered the locomotion of the four legs. This LCE body was also demonstrated to have different types of behaviors including random or directional walking, rotation or jumping. Using a similar method, a microgripper also made of azobenzene-containing LCE inspired by the hominid-type hand was able to capture different microscopic objects under a light stimulus [118]. Although azobenzene functional groups have been demonstrated to have good biocompatibility, the light wavelength that can trigger deformation of azobenzene-containing LCEs falls within the visible light range (400–700 nm) [119,120]. Visible light has poor penetration ability in the tissue, which may result in limited application of deformable scaffolds prepared by azobenzene-containing LCEs in cell and tissue engineering.

Apart from the photochromic functional groups in the polymer monomers, some nanoparticles, such as gold nanorods (AuNRs) [121] and Fe_3O_4 nanoparticles, were also introduced as the heating element in the photoresist system for achieving light-response and thus conversion of light into heat energy. The light-responsive mechanism is based on the dissipation of energy from light into heat through these dopants. For example, for our research group, Chen et al. [101] introduced AuNRs into an LCE matrix for the fabrication of several 3D microstructures. At a wavelength of 810 nm, the photon energy could be effectively converted into heat energy. The two arms of the microclamp could move toward the middle location under the stimulus of NIR light, which proved promising to work as microarms for clamping or gripping small items. The distance between the two arms is about 15 μm, which would be used to manipulate a single cell for biomedical application. Poly (*N*-isopropylacrylamide) (poly(N-isopropylacrylamide) [PNIPAAm]) has been widely used for research studies of thermo-responsive polymers. Their chains have a reversible lowest critical solution temperature (LCST) phase transition from a swollen, hydrated state to a shrunken and hydrophobic one [79]. An increase in temperature above LCST leads to the expelling of absorbed water in PNIPAAm chains, resulting in the phase separation and volume shrinkage [122]. Zheng et al. [78] introduced Fe_3O_4 nanoparticles into the photoresist system of *N*-isopropylacrylamide (NIPAM) and PEGDA and fabricated a double-armed NIR-light strip of only ~26 μm. Black Fe_3O_4 nanoparticles were found to be highly effective photothermal dopants triggered by NIR light [123]. The photothermal effect was remarkable with a very fast response time of about 0.033 s under NIR light with a power of 29.2 mW.

The photothermal effect induced by nanoparticles has attracted lot of research interest in the biomedical fields, especially in photothermal therapy for cancer and tumor diseases. However, such a photothermal effect cannot be ignored, because the extra heat due to the incorporated nanoparticles in the light-responsive photoresist could cause a temperature rise, leading to its unsuitability for the constant temperature environment of cell culture and tissue regeneration. Therefore, it would be crucial to confine the nanoparticle concentration in the light-responsive photoresists within a suitable range.

3.2.3 Electromagnetic field-responsive photoresists

In remote manipulation of the locomotion of micro/nano-devices, it may be difficult to conduct light actuation in

some opaque scaffolds or liquid environments. Electromagnetic actuation is considered as another promising method compared with light actuation due to its large actuation force in different media with low or high light transparency. Most approaches for electromagnetic actuation are involved in the incorporation of magnetite nanoparticles such as Fe_3O_4 into the prepolymerized photoresist [124] or modification of the micro/nano-structures with a thin Ni layer via surface metallization modification techniques, such as e-beam evaporation [125]. For example, Suter et al. [102] prepared a magnetic polymer composite consisting of SU-8 photoresist and Fe_3O_4 nanoparticles for subsequent TPP fabrication. A helical microswimmer and cube were fabricated using the composite with 2 vol% Fe_3O_4 nanoparticle concentration. Stimulated by a uniform rotating magnetic field, superparamagnetic helical microstructures could complete cork-screw swimming behavior for about 12 μm (forward plus drift motion) during 4 s in water. Moreover, the composite with up to 10 vol% Fe_3O_4 nanoparticles was found not to influence the cell viability of NHDFs. These 3D magnetic-field-driven microstructures could serve as microrobots for target drug delivery platforms in the complex human body liquid environment. However, due to agglomeration of the Fe_3O_4 nanoparticles induced by the van der Waals interactions, it became very difficult to achieve a high nanoparticle concentration and homogenous dispersion in the composite photoresist. Thus, surface functionality and coating were generally required to overcome such limitations.

Although the helical structures have shown remarkable advantages in magnetic actuation, the capability of cell and drug loading within the structures remains limited because of their low surface area. Porous scaffolds have been demonstrated to improve the transport efficiency. Kim et al. [103] reported a 3D porous microniche using the photoresist of SU-8 by means of TPP. Then a 150 nm Ni layer and a 20 nm Ti layer were deposited on a polymer scaffold for generating a magnetic and biocompatible microrobot. Hexahedral microrobots and cylindrical microrobots were both designed to study their magnetic moments. They found that a cylindrical structural design was favorable for minimizing the resistive force against manipulation under the actuation magnetic field of 800 mT m^{-1}. Moreover, after a 96 h culture of human embryonic kidney (HEK) 293 cells, the porous microrobots with customized pore sizes indicated good cell behavior, including attachment, migration and proliferation. In another research study, Li et al. [126] fabricated burr-like porous spherical microrobots with diameters ranging from 70 to 90 μm using a method similar to that of Kim et al. [103].

Generally, most photoresists can be incorporated with magnetite nanoparticles for achieving magnetic field actuation. Due to the bi-stimulus-responsive function of the Fe_3O_4 nanoparticles triggered by light and magnetic field simultaneously, it is believed that more advanced microactuators based on light-magnetic field responses will be further developed for biomedical applications. Multiple-stimulus-responsive photoresists deserve to be developed largely due to their outstanding functions in different situations. Recently, several studies have been reported to endow the photoresist with combined pH- and temperature-responsive behavior by employing acrylic acid and PNIPAAm as monomers. Based on these well-known stimulus-responsive monomers, Zarzar et al. [127] fabricated micropillar arrays which displayed independent responsiveness to the respective stimulus. A small temperature change and pH value could lead to large bending angles of the micropillars. Recently, Jin and co-workers [128] also reported reconfigurable compound micromachines which possessed a rapid and reversible 3D-to-3D shape deformation in response to changes in temperature and pH values.

4 TPP for medical applications

4.1 Cell engineering

Living cells in the body are typically sensitive to their surrounding microenvironment with physicochemical features including surface roughness ranging from nano- to micrometers and stiffness. In the field of cell engineering, the realization of culture conditions is of critical significance for the investigation of cell behavior such as cell growth, proliferation, alignment and colonization. Many studies have suggested that specific cell behavior can be *in vitro* resembled and investigated by mimicking the corresponding *in vivo* culture conditions using different strategies [129,130]. TPP technology has allowed researchers to control the surface topography at the multiscale for investigation of the cell–substrate interaction.

Cell alignment plays a vital role in cell behavior, which has shown remarkable influence in tissue functionality [131], strongly influenced by the 3D topography rather than a single cell level. Grigoropoulos et al. [132]

prepared a series of well-designed microstructures, including aligned high aspect ratio fibers between two glass plates, patterned ridges and grooved surfaces [133] using non-toxic ORMOCER®. The alignment of fibroblast cell lines (NIH-3T3) and epithelial cell lines (MDCK) could be controlled by changing the distance of the adjacent fibers. They found that MDCK cells should have a stronger adherence force to the fiber than the NIH-3T3 cells. They also compared the cell alignment on the orthogonally ridge-patterned surfaces with small differences of height and found that NIH-3T3 cell elongation was enhanced by increasing the ridge height. The threshold obstacle height for obtaining cell alignment was found to be about 1 μm. Similarly, Engelhardt et al. [26] reported the fabrication of a gelatin methacrylamide polymeric substrate containing a series of ridges of 1 μm width, 2 μm height and a separation of 4 μm for cell studies. The ridge-patterned substrates also exerted influence on cell alignment. To evaluate the cell alignment direction, chondrocytes were seeded on the substrates. Compared with culture petri dishes, chondrocytes were strongly aligned along the direction of the gelatin lines.

Investigation of cell migration is very important in pathological and physiological processes, such as the formation of cancer metastasis, blood vessel formation and inflammatory response [134]. Particularly in the field of tumor invasiveness, the degree of cancer malignancy was evaluated by the ability of tumor cells to invade the surrounding cells or tissues [135]. Initially, the mechanisms and regulations of cell migration were not fully understood because most studies were performed on 2D substrate models. However, the real growth of cells in the human body is a 3D multiscale microenvironment. To address this problem, Tayalia and coworkers [136] prepared a 3D microstructure with precisely controlled parameters using TPP for investigating controlled cell adhesion and migration behavior. In this work, interconnected woodpile structures with different lateral pore sizes were fabricated by a mixture photoresist composed of tris(2-hydroxy ethyl)isocyanurate triacrylate (SP499) and ethoxylated (6) trimethylol-propane triacrylate (SR499). Aided by commercial 3D imaging software, HT1080 fibrosarcoma cells showed a higher migration speed in this 3D woodpile scaffold than that in the 2D substrate. Furthermore, different pore sizes in the 3D matrix structures also changed the cell migration speed.

In addition, 3D structures prepared by TPP can be used to mechanically stimulate cell behavior, while local traction forces exerted by cells can deform these elastic structures. It is worth mentioning that the scaffolds fabricated by TPP can be used to measure traction forces produced by single cells. The measurement of contraction forces is of paramount importance for the investigation of their influence on the mechanical properties and functions of stretchable tissues. Particularly, the contraction forces of cardiomyocyte and neurite have been measured by utilizing the deformability of TPP structures [137,138]. Similar to the topographic complexity in *in vivo* 3D ECM, a 3D cobweb-like structure based on 15 μm-height pillars connected by beams of varying diameter was fabricated using OrmoComp® photoresist to measure cardiomyocyte force by Klein et al. [137]. During the fabrication, it was proven that the 3D structures could be tuned over a wide range of dimensions and the beam stiffness could be easily and accurately manipulated. Taking advantages of atomic force microscopy and time-lapse microscopy, the contraction forces by single cardiomyocytes were analyzed quantitatively for the first time. This work offers the possibility to explore the mechanical control of different types of cell growth by TPP technology. Concerning neural tissue engineering, Marino et al. [138] prepared sub-micrometric patterned substrates based on aligned ridges by biomimicking the axonal outgrowth and guidance environment. Using scanning probe techniques, an elongated PC12 neurite was estimated to exert a force of about 3 nN for bending of the ridge.

Micro/nano-stimulus-responsive actuators have been found to be useful for capturing microparticle and cell manipulation in the biomedical field. The use of stimulus-responsive photoresists for TPP has facilitated development of different micro/nano-actuators. Recently, Li et al. [139] reported a pH-triggered soft microgripper (<100 μm) with four fingers using a poly (acrylic acid)-based hydrogel for capturing microparticles and cells. As discussed above, carboxyl (–COOH) in the side chain played an important role in the deformation triggered by a pH value change. When the pH value was changed to be lower than 9, the straight fingers would bend to grip a target. However, the sequent cell culture indicated that the catching procedure did little harm to the cells.

Therapeutic cell delivery to target disease situations is a potential treatment for some diseases such as neurodegenerative diseases. However, it remains challenging to complete the targeted transportation of cells and subsequent *in situ* differentiation in current clinic applications. Micro/nano-robots loaded with therapeutic cells display enormous advantages in performing therapeutic tasks [140]. Dong et al. [141] prepared 3D helical magnetoelectric microswimmers via TPP to deliver

neuron-like cells. These helical structures were prepared using gelatin-methacryloyl as monomers and P2CK as the PI by TPP. More importantly, gelatin-methacryloyl could be degraded by the enzymes generated by the cells. After incubation in water containing magneto-electric nanoparticles composed of a $CoFe_2O_4$ (CFO) core and a $BiFeO_3$ (BFO) shell, magneto-electric microswimmers were produced. When SH-SY5Y cells were cultured on the microswimmers using an alternating magnetic field, the whole structures gradually collapsed as time passed by. Moreover, obvious neuronal differentiation was observed by testing relevant protein formation after 7 days. Although this work demonstrated the possibility of the potential value of micro/nano-robots in neurodegenerative diseases, a large number of therapeutic cells were required for such a therapy method. As the helical structures had only a low surface area, more effort would be needed to enhance the micro/nano-structures with more efficient cell loading ability.

4.2 Tissue engineering

Tissue engineering is recognized as an interdisciplinary field of research that applies material and biological science to create artificial organ and tissue substrates [142]. 3D scaffolds function as the desirable skeleton for the development of drug-loaded cells and further promotion of tissue formation. Therefore, it is essential for the scaffolds to mimic the natural ECM structures of the target tissues. The peculiar features offered by the TPP technique have enabled the preparation of versatile 3D structures with precisely defined interconnected pores and topographical stimulation *in vitro* on the microscale and nanoscale for specific tissue formation. Currently, various types of tissue engineering research studies, such as retina, heart, bone and cartilage tissue, have been carried out based on the scaffolds prepared via TPP. Nevertheless, highly engineered scaffolds with specific features and functions are in great demand for biomedical applications.

Degenerative retinal diseases are important health matters that are urgently needed to be solved by new and reliable therapeutic methods because of the limitation of current strategies and the shortage of substrates from donors. Because photoreceptor cells are tightly packed and aligned with the path of light entering the eye, the scaffolds used in retinal tissue repair require sophisticated multilayered structures [143]. Tucker et al. [94] prepared an innovative 3D hexagonal scaffold with interconnected horizontal pores for oxygen and nutrient element delivery, and with closely packed vertical pores of varying size for facilitating the growth of human induced pluripotent stem cell (iPSC)-derived retinal progenitor cells (RPCs) loaded in commercially available IP-S photoresists. By tuning the slicing distance and hatching distance, the printing time and design-to-structure fidelity were optimized for fabricating larger scaffolds. The expression of neural progenitor-specific protein TUJ1 aligned in the vertical pores demonstrated the successful transplantation and correct cell orientation of RPCs into the scaffold. Recently, they used poly (caprolactone) (PCL) modified by acrylate groups to prepare similar degradable photoreceptor cell delivery scaffolds [144]. In this work, for improving the design-to-structure fidelity, different formulations of PCL functioned by various numbers of acrylate groups per prepolymer molecule were explored except the aforementioned printing parameters. After staining by the nuclear marker DAPI, it was demonstrated that RPCs successfully grew and proliferated in the pores, which further indicated that they could be transported to the target site of the eye with little influence of the shear forces in surgery because of the protection of the interconnected scaffold. Most importantly, when the cell-free scaffolds were implanted into the sub-retinal space of a pig model, no inflammation, infection and tumor formation were detected after 1 month. Therefore, therapy based on a porous 3D scaffold via TPP would provide a robust, promising and repeatable tool for photoreceptor cell replacement for those suffering from late-stage retinal degeneration.

TPP has also shown great advantages in the creation of microstructured scaffolds made of biodegradable polymers for bone defect repair. Among diverse biodegradable polymers, synthetic polylactic acid (PLA)-based copolymers are the most widely used for bone tissue engineering because of their tunable mechanical properties [145]. Timashev et al. [146] synthesized star-shape methacrylate functionalized poly(D,L-lactide) for fabricating 3D porous scaffold structures composed of two layers of hollow cylinder arrays in a hexagonal arrangement. Young's modulus and microhardness were found to be 4.11 and 0.36 GPa, respectively, which are comparable to that of human bone. This scaffold was demonstrated to provide human mesenchymal stem cells with a suitable environment *in vitro* for cell growth and further differentiation toward the osteogenic lineage without osteogenic stimulation. In another work, Hauptmann and coworkers [147] fully explored how the monomer ratio of poly(D,L-lactide) and poly-ε-caprolactone

influenced the elastic modulus and provided a material platform for bone and cartilage reconstruction in combination with the TPP lithography technique. With a ratio of 2:8, the Schwarz primitive scaffold showed very good performance as an artificial tumor environment.

In order to reduce the immune rejection and chronic inflammation after the scaffold implantation, drugs were generally needed to be incorporated in the scaffolds and released on demand for reducing some side effects. Dexamethasone is a widely used pharmaceutical agent which not only can solve the aforementioned problems but also stimulate the differentiation of osteogenic cells in bone tissue engineering [148,149]. Paun et al. [150] reported electrically responsive microreservoirs with tunable dexamethasone release kinetics. Vertical microtubes arrays were first fabricated using IP-L780 photoresist via TPP, then loaded with a polypyrrole/dexamethasone film by an immersion process. Polypyrrole is a kind of conductive polymer and its intrinsic conductivity can stimulate the growth of bone tissue. Under the stimulation of electrical field, the drug can be released from the redox polymer film because of the electrical switching of the polymer redox states [151]. Using a voltage cycle between −1 V and +1 V, dexamethasone could be released at the desired time. Meanwhile, the osteogenic efficiency of osteoblast-like MG-63 using electrically responsive microreservoirs was improved by 2.2 times as compared to that using unstimulated samples.

4.3 Biomedical devices

With the aforementioned advantages, TPP offers highly efficient reproduction of small-scale 3D medical devices with micro- or nano-features, including microneedles for drug delivery, microfluidic systems and biosensors. Some microneedles require complex shape and small tip angle for low microneedle penetration forces. Gittard et al. [152] fabricated round-tip microneedle arrays made of a photoreactive acrylate-based polymer by using TPP and polydimethylsiloxane (PDMS) micromolding. First, a master structure for a solid microneedle array with a height of 500 μm and a base diameter of 150 μm was fabricated via TPP. Subsequently, a negative mold was fabricated using PDMS based on the master structure. Finally, a number of microneedle arrays could be cast using the negative mold. The microneedle arrays could maintain their elastic deformation over a 10 N axial load and successfully created pores in human stratum corneum and epidermis. Recently, Balmert et al. [37] first prepared dissolving undercut microneedle arrays as cutaneous vaccine delivery platforms with tip-loaded antigen plus adjuvant vaccine components using a similar method. In this work, a square pyramid head (250 μm × 250 μm base area) was designed to increase skin insertion for delivering inside biological cargos. Importantly, cutaneous vaccination with antigen-loaded microneedle arrays could simultaneously deliver adjuvant and antigen to the same skin microenvironment, which further triggered more potent antigen-specific immune responses than conventional immunization by intramuscular injection. These studies indicate that TPP enabled fast reproduction of microneedles, which would facilitate the use of microneedles for future clinical application.

Different microfluidic components have been created for lab-on-a-chip applications. Kumi et al. [153] reported the fabrication of large-area microfluidic master structures via high-speed TPP. They used FLUOR-SU8 to fabricate master relief structures with different cross-sections and features with a high aspect ratio for the PDMS molds. This technology has been useful to prepare microfluidic structures that are challenging to fabricate using conventional photolithographic methods, including microfluidic channels with non-rectangular cross-sections. Micropumps fabricated by stimulus-responsive hydrogel materials have attracted a growing interest in bioanalytical areas. Xiong et al. [154] fabricated a solvent-driven micropump made of solvent-responsive polyacrylamide hydrogel. The micropump system was composed of a hydrogel valve, a microfluidic channel and a hydrogel film wall. When the solvent was changed from water to solvent, the 2.5 μm-thick hydrogel film wall would bend to trigger the closed and open state of the hydrogel valve. A fluid change of 9.2×10^{-2} pL in the microchannel was completed in only 0.17 s. Thus, the micropump would have a great potential in achieving ultra-microdosage drug release *in vivo*.

It is also possible to produce other stimulus-responsive microscale actuators via TPP. Zheng et al. [78] introduced Fe_3O_4 nanoparticles by a surface-modifier to the mixture of poly(*N*-isopropylacrylamide) (PNIPAAm) and PEGDA for fabricating a double-armed NIR-light hydrogel actuator with only ~26 μm thick. Two arms in this microdevice could close and open to achieve a very fast response time of about 0.033 s in response to NIR light with a power of 29.2 mW. The biocompatibility and small size rendered its potential application in the biomedical MEMS field. It is worth noting that Fe_3O_4

nanoparticles can also respond to a magnetic field, which is expected to be actuated under multiple external stimuli. In a previous work, this group reported a 3D hydrogel micronail with a size of only ~10 μm which consisted of a rod and a cap out of surface-modified Fe_3O_4 nanoparticles and magnetic gelphotoresists [104]. The rod part could be reversely deformed to a wide angle of 52.4° under a magnetic field. Taking the biodegradability into consideration, Wang et al. [155] fabricated enzymatically biodegradable magnetic-field-driven soft helical microswimmers based on a protein photoresist by means of TPP. Gelatin methacryloyl (GelMA), which is highly cytocompatible and bioactive, is often used as a material for cell culture. For instance, GelMA and photoinitiator P2CK were first polymerized into helical microstructures, followed by a decoration with magnetite (Fe_3O_4) nanoparticles in water. Under a rotating magnetic field, the soft microswimmers had some advantages with respect to the forward velocity and drift velocity as compared to other rigid helical microswimmers. The helical structures also showed better human skin fibroblast cell attachment performance. Moreover, the GelMA microswimmers could be degraded by cell-secreted proteases after a 1-week culture of HaCaT cells, providing opportunities for the next generation of target site therapy using biodegradable small robots.

5 Summary, current challenges and future perspectives

This paper presents a comprehensive review of the properties of widely used PIs and photoresists which play crucial roles for designing and developing stimulus-responsive micro/nano-structures for biomedical applications via the TPP nanolithography technology. Due to significance of water-soluble PIs in biomedical fields, the properties of the traditional commercial and newly emerging PIs are also described. Moreover, the design and synthesis principles of the PIs are summarized with respect to TPA cross section and water solubility. Most importantly, stimulus-responsive materials can offer the 3D micro/nano-structures "life" with changeable properties in a controllable approach, which cannot be achieved by the static type of micro/nano-structures. With the availability of different PIs, various types of stimulus-responsive photoresists facilitating the generation of enormous 3D micro/nano-structures via TPP for various biomedical applications, such as cell engineering, tissue engineering and medical devices, are also described. As reflected from a number of distinctive recent TPP-related works, the TPP technology has been demonstrated to possess many advantages in producing well-defined 3D structures over conventional miniaturization fabrication technology, including high spatial resolution, easy handling, repeatability and ample material choice.

Despite the aforesaid advantages, TPP as a powerful and versatile 3D micro/nano-fabrication tool still exhibits certain drawbacks and challenges, which need to be addressed in future work. For the most unique feature of the TPP known as the submicron-size voxel, a long printing time is generally needed for producing millimeter-scale structures, which may hinder its application to mass manufacturing. Moreover, the voxel-to-voxel printing method makes the final sample have inevitable connection gaps, which are especially obvious in some unstable photoresists in the development process. Furthermore, the biomaterial choice for the preparation of 3D scaffolds used as soft tissues such as muscle and retina remains limited. Although hydrogels are widely used candidate materials in cell engineering and tissue engineering, 3D hydrogel scaffolds prepared by TPP exhibit a low spatial resolution because of their high water content. Precise manipulation of the topography and pore dimensions at the nanoscale is still difficult to achieve. Particularly, the absence of suitable PIs for TPP nanolithography with a high efficiency in aqueous solution remains a great barrier for the fabrication 3D hydrogel micro/nano-structures for biomedical applications.

Recently, some of these challenges have been mitigated. For instance, the special resolution of TPP can be improved by modification of the scanning speed and laser power. Therefore, highly efficient aqueous-based PIs or monomers with photoactive moieties were developed to optimize the two parameters [49]. A host–guest chemical reaction was proposed to prepare water soluble PIs with high efficiency for polymerization in an aqueous medium [66,67,69,72,156]. To address the time-consuming issue, the recent TPP printing equipment has been enhanced with faster scanning technologies [157]. Another more efficient and effective strategy for the TPP is the application of an array for preparing periodic constructs and multi-microfabrication [158,159], so as to enable a series of small microlenses to be produced in one pass. New biocompatible and biodegradable photopolymerizable materials are being enriched so that users can create novel micro/nano-structures with the industry-standard CAD software. With this vision, it is evident that TPP potentially would solve many current challenges in conventional

technologies in regard to spatial resolution. In order to realize its full range of capabilities, it is expected that the photopolymerizable material pool and water-soluble TPP PIs can be further developed.

Acknowledgements: The work described in this paper was mainly supported by the funding support to the State Key Laboratories in Hong Kong from the Innovation and Technology Commission (ITC) of the Government of the Hong Kong Special Administrative Region (HKSAR), China. The authors would like to express their sincere thanks for the financial support from the Research Committee of The Hong Kong Polytechnic University (Project code: BBX5, BBXC, RK28 and G-YBRM)

Conflict of interest: The authors declare no conflict of interest regarding the publication of this paper.

References

[1] Nikkhah M, Edalat F, Manoucheri S, Khademhosseini A. Engineering microscale topographies to control the cell–substrate interface. Biomaterials. 2012;33:5230–46.

[2] Chen G, Dong C, Yang L, Lv Y. 3D scaffolds with different stiffness but the same microstructure for bone tissue engineering. ACS Appl Mater Interfaces. 2015;7:15790–802.

[3] Nakonieczny DS, Antonowicz M, Paszenda ZK. Cenospheres and their application advantages in biomedical engineering – a systematic review. Rev Adv Mater Sci. 2020;59:115–30.

[4] Qiu F, Nelson BJ. Magnetic helical micro- and nanorobots: toward their biomedical applications. Engineering 2015;1:21–6.

[5] Liu C. Rapid fabrication of microfluidic chip with three-dimensional structures using natural lotus leaf template. Microfluidics Nanofluidics. 2010;9:923–31.

[6] Ren X, Han Y, Wang J, Jiang Y, Yi Z, Xu H, et al. An aligned porous electrospun fibrous membrane with controlled drug delivery – an efficient strategy to accelerate diabetic wound healing with improved angiogenesis. Acta Biomater. 2018;70:140–53.

[7] Zang S, Chang S, Shahzad MB, Sun X, Jiang X, Yang H. Ceramics-based drug delivery system: A review and outlook. Rev Adv Mater Sci. 2019;58:82–97.

[8] Xiangzhou H, Zhijie Y, Senxian K, Man J, Zuowan Z, Jihua G, et al. Cellulose hydrogel skeleton by extrusion 3D printing of solution. Nanotechnol Rev. 2020;9:345–53.

[9] Sandoval JH, Soto KF, Murr LE, Wicker RB. Nanotailoring photocrosslinkable epoxy resins with multiλwalled carbon nanotubes for stereolithography layered manufacturing. J Mater Sci. 2006;42:156–65.

[10] Lin J, Ding B, Yang J, Yu J, Sun G. Subtle regulation of the micro- and nanostructures of electrospun polystyrene fibers and their application in oil absorption. Nanoscale. 2012;4:176–82.

[11] Wang SX, Yap CC, He J, Chen C, Wong SY, Li X. Electrospinning: a facile technique for fabricating functional nanofibers for environmental applications. Nanotechnol Rev. 2016;5:51–73.

[12] Nguyen AK, Narayan RJ. Two-photon polymerization for biological applications. Mater Today. 2017;20:314–22.

[13] Eschenbaum C, Großmann D, Dopf K, Kettlitz S, Bocksrocker T, Valouch S, et al. Hybrid lithography: Combining UV-exposure and two photon direct laser writing. Opt Express. 2013;21:29921–6.

[14] Burmeister F, Zeitner UD, Nolte S, Tünnermann A. High numerical aperture hybrid optics for two-photon polymerization. Opt Express. 2012;20:7994–8005.

[15] Malinauskas M, Žukauskas A, Bičkauskaitė G, Gadonas R, Juodkazis S. Mechanisms of three-dimensional structuring of photo-polymers by tightly focussed femtosecond laser pulses. Opt Express. 2010;18:10209–21.

[16] Gittard SD, Miller PR, Boehm RD, Ovsianikov A, Chichkov BN, Heiser J, et al. Multiphoton microscopy of transdermal quantum dot delivery using two photon polymerization-fabricated polymer microneedles. Faraday Discuss. 2011;149:171–85; discussion 227–45.

[17] Ovsianikov A, Schlie S, Ngezahayo A, Haverich A, Chichkov BN. Two-photon polymerization technique for microfabrication of CAD-designed 3D scaffolds from commercially available photosensitive materials. J Tissue Eng Regen Med. 2007;1:443–9.

[18] Winfield RJ, O'Brien S. Two-photon polymerization of an epoxy–acrylate resin material system. Appl Surf Sci. 2011;257:5389-92.

[19] Xiong W, Zhou Y, Hou W, Jiang L, Mahjouri-Samani M, Park J, et al. Laser-based micro/nanofabrication in one, two and three dimensions. Front Optoelectron. 2015;8:351–78.

[20] Puce S, Sciurti E, Rizzi F, Spagnolo B, Qualtieri A, De Vittorio M, et al. 3D-microfabrication by two-photon polymerization of an integrated sacrificial stencil mask. Micro Nano Eng. 2019;2:70–5.

[21] Staudinger U, Zyla G, Krause B, Janke A, Fischer D, Esen C, et al. Development of electrically conductive microstructures based on polymer/CNT nanocomposites via two-photon polymerization. Microelectronic Eng. 2017;179:48–55.

[22] Jin W, Gao Y, Liu M. Fabrication of large area two-dimensional nonlinear photonic lattices using improved Michelson interferometer. Opt Commun. 2013;289:140–3.

[23] Marino A, Filippeschi C, Mattoli V, Mazzolai B, Ciofani G. Biomimicry at the nanoscale: current research and perspectives of two-photon polymerization. Nanoscale. 2015;7:2841–50.

[24] Mandt D, Gruber P, Markovic M, Tromayer M, Rothbauer M, Krayz SRA, et al. Fabrication of biomimetic placental barrier structures within a microfluidic device utilizing two-photon polymerization. Int J Bioprinting. 2018;4:144.

[25] Torgersen J, Qin X-H, Li Z, Ovsianikov A, Liska R, Stampfl J. Hydrogels for two-photon polymerization: A toolbox for mimicking the extracellular matrix. Adv Funct Mater. 2013;23:4542–54.

[26] Engelhardt S, Hoch E, Borchers K, Meyer W, Krüger H, Tovar GE, et al. Fabrication of 2D protein microstructures and 3D polymer–protein hybrid microstructures by two-photon polymerization. Biofabrication. 2011;3:025003.

[27] Liao C, Wuethrich A, Trau M. A material odyssey for 3D nano/microstructures: two photon polymerization based nanolithography in bioapplications. Applied Mater Today. 2020;19:100635.
[28] Woggon T, Kleiner T, Punke M, Lemmer U. Nanostructuring of organic-inorganic hybrid materials for distributed feedback laser resonators by two-photon polymerization. Opt Express. 2009;17:2500–7.
[29] Tromayer M, Dobos A, Gruber P, Ajami A, Dedic R, Ovsianikov A, et al. A biocompatible diazosulfonate initiator for direct encapsulation of human stem cells via two-photon polymerization. Polym Chem. 2018;9:3108–17.
[30] Lei B, Shin K-H, Noh D-Y, Jo I-H, Koh Y-H, Choi W-Y, et al. Nanofibrous gelatin–silica hybrid scaffolds mimicking the native extracellular matrix (ECM) using thermally induced phase separation. J Mater Chem. 2012;22:14133–40.
[31] Iwona C, Stefan L, Christoph A, Christoph DG. Nanomedicine in diagnostics and therapy of cardiovascular diseases: beyond atherosclerotic plaque imaging. Nanotechnol Rev. 2013;2:449–72.
[32] Kaleemullah K, Ming S. Electrospun cellulose acetate nanofibers and Au@AgNPs for antimicrobial activity – A mini review. Nanotechnol Rev. 2019;8:246–57.
[33] Limongi T, Lizzul L, Giugni A, Tirinato L, Pagliari F, Tan H, et al. Laboratory injection molder for the fabrication of polymeric porous poly-epsilon-caprolactone scaffolds for preliminary mesenchymal stem cells tissue engineering applications. Microelectronic Eng. 2017;175:12–6.
[34] Wu X, Xiao T, Luo Z, He R, Cao Y, Guo Z, et al. A micro-/nano-chip and quantum dots-based 3D cytosensor for quantitative analysis of circulating tumor cells. J Nanobiotechnol. 2018;16:1–9.
[35] Elsner JJ, Kraitzer A, Grinberg O, Zilberman M. Highly porous drug-eluting structures: From wound dressings to stents and scaffolds for tissue regeneration. Biomatter. 2012;2:239–70.
[36] Kufelt O, El-Tamer A, Sehring C, Meißner M, Schlie-Wolter S, Chichkov BN. Water-soluble photopolymerizable chitosan hydrogels for biofabrication via two-photon polymerization. Acta Biomater. 2015;18:186–95.
[37] Balmert SC, Carey CD, Falo GD, Sethi SK, Erdos G, Korkmaz E, et al. Dissolving undercut microneedle arrays for multicomponent cutaneous vaccination. J Controlled Rel. 2020;317:336–46.
[38] Ali Z, Türeyen EB, Karpat Y, Çakmakcı M. Fabrication of polymer micro needles for transdermal drug delivery system using DLP based projection stereo-lithography. Procedia Cirp. 2016;42:87–90.
[39] He GS, Tan L-S, Zheng Q, Prasad PN. Multiphoton absorbing materials: molecular designs, characterizations, and applications. Chem Rev. 2008;108:1245–330.
[40] Quentin Le T, Hervé S, Marie-Hélène D. Functionalized nanomaterials: their use as contrast agents in bioimaging: mono- and multimodal approaches. Nanotechnol Rev. 2013;2:125–69.
[41] Zhou X, Hou Y, Lin J. A review on the processing accuracy of two-photon polymerization. AIP Adv. 2015;5:030701.
[42] Tomal W, Ortyl J. Water-soluble photoinitiators in biomedical applications. Polymers. 2020;12:1073.
[43] Zhang S, Wan X, Peng Y, Yin Q. Synthesis and properties of four new two-photon polymerization initiators with expanded conjugated structures. MS&E. 2019;479:012109.
[44] Cumpston BH, Ananthavel SP, Barlow S, Dyer DL, Ehrlich JE, Erskine LL, et al. Two-photon polymerization initiators for three-dimensional optical data storage and microfabrication. Nature 1999;398:51–4.
[45] Hao F, Liu Z, Zhang M, Liu J, Zhang S, Wu J, et al. Four new two-photon polymerization initiators with varying donor and conjugated bridge: Synthesis and two-photon activity. Spectrochim Acta Part A. 2014;118:538–42.
[46] Li Z, Pucher N, Cicha K, Torgersen J, Ligon SC, Ajami A, et al. A straightforward synthesis and structure–activity relationship of highly efficient initiators for two-photon polymerization. Macromolecules. 2013;46:352–61.
[47] Li Z, Siklos M, Pucher N, Cicha K, Ajami A, Husinsky W, et al. Synthesis and structure–activity relationship of several aromatic ketone-based two-photon initiators. J Polym Sci Part A Polym Chem. 2011;49:3688–99.
[48] Torgersen J, Ovsianikov A, Mironov V, Pucher N, Qin X, Li Z, et al. Photo-sensitive hydrogels for three-dimensional laser microfabrication in the presence of whole organisms. J Biomed Opt. 2012;17:105008.
[49] Dobos A, Van Hoorick J, Steiger W, Gruber P, Markovic M, Andriotis OG, et al. Thiol–gelatin–norbornene bioink for laser-based high-definition bioprinting. Advanced Healthcare Materials. 2019;9:1900752.
[50] Dobos A, Steiger W, Theiner D, Gruber P, Lunzer M, Van Hoorick J, et al. Screening of two-photon activated photodynamic therapy sensitizers using a 3D osteosarcoma model. Analyst. 2019;144:3056–63.
[51] Zhang W, Soman P, Meggs K, Qu X, Chen S. Tuning the poisson's ratio of biomaterials for investigating cellular response. Adv Funct Mater. 2013;23:3226–32.
[52] Crowe J, El-Tamer A, Nagel D, Koroleva A, Madrid-Wolff J, Olarte O, et al. Development of two-photon polymerised scaffolds for optical interrogation and neurite guidance of human iPSC-derived cortical neuronal networks. Lab Chip. 2020;20:1792–806.
[53] Brigo L, Urciuolo A, Giulitti S, Della Giustina G, Tromayer M, Liska R, et al. 3D high-resolution two-photon crosslinked hydrogel structures for biological studies. Acta Biomater. 2017;55:373–84.
[54] Jhaveri SJ, McMullen JD, Sijbesma R, Tan L-S, Zipfel W, Ober CK. Direct three-dimensional microfabrication of hydrogels via two-photon lithography in aqueous solution. Chem Mater. 2009;21:2003–6.
[55] Ovsianikov A, Deiwick A, Van Vlierberghe S, Pflaum M, Wilhelmi M, Dubruel P, et al. Laser fabrication of 3D gelatin scaffolds for the generation of bioartificial tissues. Materials. 2011;4:288–99.
[56] Basu S, Rodionov V, Terasaki M, Campagnola PJ. Multiphoton-excited microfabrication in live cells via Rose Bengal cross-linking of cytoplasmic proteins. Opt Lett. 2005;30:159–61.
[57] Billiet T, Gevaert E, De Schryver T, Cornelissen M, Dubruel P. The 3D printing of gelatin methacrylamide cell-laden tissue-engineered constructs with high cell viability. Biomaterials. 2014;35:49–62.

[58] Qin XH, Torgersen J, Saf R, Mühleder S, Pucher N, Ligon SC, et al. Three-dimensional microfabrication of protein hydrogels via two-photon-excited thiol-vinyl ester photopolymerization. J Polym Sci Part A: Polym Chem. 2013;51:4799–810.
[59] Ovsianikov A, Mühleder S, Torgersen J, Li Z, Qin X-H, Van Vlierberghe S, et al. Laser photofabrication of cell-containing hydrogel constructs. Langmuir. 2014;30:3787–94.
[60] Wan X, Zhao Y, Xue J, Wu F, Fang X. Water-soluble benzylidene cyclopentanone dye for two-photon photopolymerization. J Photochem Photobiol A Chem. 2009;202:74–9.
[61] Tromayer M, Gruber P, Markovic M, Rosspeintner A, Vauthey E, Redl H, et al. A biocompatible macromolecular two-photon initiator based on hyaluronan. Polym Chem. 2017;8:451–60.
[62] Tomatsu I, Peng K, Kros A. Photoresponsive hydrogels for biomedical applications. Adv Drug Delivery Rev. 2011;63:1257–66.
[63] Wang X, Wei Z, Baysah CZ, Zheng M, Xing J. Biomaterial-based microstructures fabricated by two-photon polymerization microfabrication technology. RSC Adv. 2019;9:34472–80.
[64] Day A, Arnold AP, Blanch RJ, Snushall B. Controlling factors in the synthesis of cucurbituril and its homologues. J Org Chem. 2001;66:8094–100.
[65] Thomas SS, Tang H, Bohne C. Noninnocent role of Na + ions in the binding of the n-phenyl-2-naphthylammonium cation as a ditopic guest with cucurbit [7] uril. J Am Chem Soc. 2019;141:9645–54.
[66] Huang Z, Qin K, Deng G, Wu G, Bai Y, Xu J-F, et al. Supramolecular chemistry of cucurbiturils: tuning cooperativity with multiple noncovalent interactions from positive to negative. Langmuir. 2016;32:12352–60.
[67] Tang H, Fuentealba D, Ko YH, Selvapalam N, Kim K, Bohne C. Guest binding dynamics with cucurbit [7] uril in the presence of cations. J Am Chem Soc. 2011;133:20623–33.
[68] Guo Y, Guo S, Ren J, Zhai Y, Dong S, Wang E. Cyclodextrin functionalized graphene nanosheets with high supramolecular recognition capability: synthesis and host–guest inclusion for enhanced electrochemical performance. ACS Nano. 2010;4:4001–10.
[69] Xing J-F, Zheng M-L, Duan X-M. Two-photon polymerization microfabrication of hydrogels: an advanced 3D printing technology for tissue engineering and drug delivery. Chem Soc Rev. 2015;44:5031–39.
[70] Xing J, Liu J, Zhang T, Zhang L, Zheng M, Duan X. A water soluble initiator prepared through host–guest chemical interaction for microfabrication of 3D hydrogels via two-photon polymerization. J Mater Chem B. 2014;2:4318–23.
[71] Gu J, Yulan W, Chen W-Q, Dong X-Z, Duan X-M, Kawata S. Carbazole-based 1D and 2D hemicyanines: synthesis, two-photon absorption properties and application for two-photon photopolymerization 3D lithography. N J Chem. 2007;31:63–8.
[72] Zheng Y-C, Zhao Y-Y, Zheng M-L, Chen S-L, Liu J, Jin F, et al. Cucurbit [7] uril-carbazole two-photon photoinitiators for the fabrication of biocompatible three-dimensional hydrogel scaffolds by laser direct writing in aqueous solutions. ACS Appl Mater Interfaces. 2019;11:1782–9.
[73] Farsari M, Chichkov BN. Two-photon fabrication. Nat Photonics. 2009;3:450–2.
[74] Stoneman M, Fox M, Zeng C, Raicu V. Real-time monitoring of two-photon photopolymerization for use in fabrication of microfluidic devices. Lab Chip. 2009;9:819–27.
[75] Liu Y, Campbell JH, Stein O, Jiang L, Hund J, Lu Y. Deformation behavior of foam laser targets fabricated by two-photon polymerization. Nanomaterials. 2018;8:498.
[76] Schlie S, Ngezahayo A, Ovsianikov A, Fabian T, Kolb H-A, Haferkamp H, et al. Three-dimensional cell growth on structures fabricated from ORMOCER® by two-photon polymerization technique. J Biomater Appl. 2007;22:275–87.
[77] Ostendorf A, Chichkov BN. Two-photon polymerization: a new approach to micromachining. Photonics Spectra. 2006;40:72.
[78] Zheng C, Jin F, Zhao Y, Zheng M, Liu J, Dong X, et al. Light-driven micron-scale 3D hydrogel actuator produced by two-photon polymerization microfabrication. Sens Actuators B Chem. 2020;304:127345.
[79] Hippler M, Blasco E, Qu J, Tanaka M, Barner-Kowollik C, Wegener M, et al. Controlling the shape of 3D microstructures by temperature and light. Nat Commun. 2019;10:1–8.
[80] Carlotti M, Mattoli V. Functional materials for two-photon polymerization in microfabrication. Small. 2019;15:1902687.
[81] Lee MR, Phang IY, Cui Y, Lee YH, Ling XY. Shape-shifting 3D protein microstructures with programmable directionality via quantitative nanoscale stiffness modulation. Small. 2015;11:740–8.
[82] Kopeček J. Hydrogel biomaterials: a smart future?. Biomaterials. 2007;28:5185–92.
[83] Shahsavan H. Liquid Crystal Networks for Smart Biomimetic Micro/nano Structured Adhesives; 2017.
[84] McCracken JM, Tondiglia VP, Auguste AD, Godman NP, Donovan BR, Bagnall BN, et al. Liquid crystalline elastomers: microstructured photopolymerization of liquid crystalline elastomers in oxygen-rich environments (Adv. Funct. Mater. 40/2019). Adv Funct Mater. 2019;29:1970274.
[85] Ming L, Zhen C, Haibao L, Kai Y. Recent progress in shape memory polymer composites: methods, properties, applications and prospects, Nanotechno Rev. 2019;8:327–51.
[86] Ohm C, Brehmer M, Zentel R. Liquid crystalline elastomers as actuators and sensors. Adv Mater. 2010;22:3366–87.
[87] Ahmed A, Wang X, Yang M. Biocompatible materials of pulsatile and rotary blood pumps: A brief review. Rev Adv Mater Sci. 2020;59:322–39.
[88] Martella D, Parmeggiani C. Advances in cell scaffolds for tissue engineering: the value of liquid crystalline elastomers. Chem – Eur J. 2018;24:12206–20.
[89] Ferrantini C, Pioner JM, Martella D, Coppini R, Piroddi N, Paoli P, et al. Development of light-responsive liquid crystalline elastomers to assist cardiac contraction. Circulation Res. 2019;124:e44–54.
[90] Schmid M, Ludescher D, Giessen H. Optical properties of photoresists for femtosecond 3D printing: refractive index, extinction, luminescence-dose dependence, aging, heat treatment and comparison between 1-photon and 2-photon exposure. Opt Mater Express. 2019;9:4564–77.
[91] Larramendy F, Yoshida S, Maier D, Fekete Z, Takeuchi S, Paul O. 3D arrays of microcages by two-photon lithography for spatial organization of living cells. Lab Chip. 2019;19:875–84.

[92] Lemma ED, Spagnolo B, Rizzi F, Corvaglia S, Pisanello M, De Vittorio M, et al. Microenvironmental stiffness of 3D polymeric structures to study invasive rates of cancer cells. Adv Healthc Mater. 2017;6:1700888.
[93] Accardo A, Blatché MC, Courson R, Loubinoux I, Thibault C, Malaquin L, et al. Multiphoton direct laser writing and 3D imaging of polymeric freestanding architectures for cell colonization. Small. 2017;13:1700621.
[94] Worthington KS, Wiley LA, Kaalberg EE, Collins MM, Mullins RF, Stone EM, et al. Two-photon polymerization for production of human iPSC-derived retinal cell grafts. Acta Biomater. 2017;55:385–95.
[95] Hwang G, Decanini D, Leroy L, Haghiri-Gosnet A. Note: On-chip multifunctional fluorescent-magnetic Janus helical microswimmers. Rev Sci Instrum. 2016;87:036104.
[96] Knoška J, Adriano L, Awel S, Beyerlein KR, Yefanov O, Oberthuer D, et al. Ultracompact 3D microfluidics for time-resolved structural biology. Nat Commun. 2020;11:1–12.
[97] Lay CL, Lee MR, Lee HK, Phang IY, Ling XY. Transformative two-dimensional array configurations by geometrical shape-shifting protein microstructures. ACS Nano. 2015;9:9708–17.
[98] Wei S, Liu J, Zhao Y, Zhang T, Zheng M, Jin F, et al. Protein-based 3d microstructures with controllable morphology and pH-responsive properties. ACS Appl Mater Interfaces. 2017;9:42247–57.
[99] Scarpa E, Lemma ED, Fiammengo R, Cipolla MP, Pisanello F, Rizzi F, et al. Microfabrication of pH-responsive 3D hydrogel structures via two-photon polymerization of high-molecular-weight poly(ethylene glycol) diacrylates. Sens Actuators B: Chem. 2019;279:418–26.
[100] Zeng H, Wasylczyk P, Parmeggiani C, Martella D, Burresi M, Wiersma DS. Light-fueled microscopic walkers. Adv Mater. 2015;27:3883–7.
[101] Chen L, Dong Y, Tang C-Y, Zhong L, Law W-C, Tsui GC, et al. Development of direct-laser-printable light-powered nanocomposites, ACS Appl Mater Interfaces. 2019;11:19541–53.
[102] Suter M, Zhang L, Siringil EC, Peters C, Luehmann T, Ergeneman O, et al. Superparamagnetic microrobots: fabrication by two-photon polymerization and biocompatibility. Biomed Microdevices. 2013;15:997–1003.
[103] Kim S, Qiu F, Kim S, Ghanbari A, Moon C, Zhang L, et al. Fabrication and characterization of magnetic microrobots for three-dimensional cell culture and targeted transportation, Adv Mater. 2013;25:5863–68.
[104] Xiong Z, Zheng C, Jin F, Wei R, Zhao Y, Gao X, et al. Magnetic-field-driven ultra-small 3D hydrogel microstructures: preparation of gel photoresist and two-photon polymerization microfabrication. Sens Actuators B: Chem. 2018;274:541–50.
[105] Buenger D, Topuz F, Groll J. Hydrogels in sensing applications. Prog Polym Sci. 2012;37:1678–719.
[106] Li R, Wu Z, Wangb Y, Ding L, Wang Y. Role of pH-induced structural change in protein aggregation in foam fractionation of bovine serum albumin. Biotechnol Rep. 2016;9:46–52.
[107] Arcaute K, Mann B, Wicker R. Stereolithography of spatially controlled multi-material bioactive poly(ethylene glycol) scaffolds. Acta Biomater. 2010;6:1047–54.
[108] Feifei J, Guoling L, Bo Y, Bing Y, Youqing S, Hailin C. Investigation of rare earth upconversion fluorescent nanoparticles in biomedical field. Nanotechno Rev. 2019;8:1–17.
[109] Kaehr B, Shear JB. Multiphoton fabrication of chemically responsive protein hydrogels for microactuation. Proc Natl Acad Sci USA. 2008;105:8850–54.
[110] Sugiura S, Szilágyi A, Sumaru K, Hattori K, Takagi T, Filipcsei G, et al. On-demand microfluidic control by micropatterned light irradiation of a photoresponsive hydrogel sheet. Lab a Chip. 2009;9:196–8.
[111] Hou M, Yang R, Zhang L, Zhang L, Liu G, Xu Z, et al. Injectable and natural humic acid/agarose hybrid hydrogel for localized light-driven photothermal ablation and chemotherapy of cancer. ACS Biomater Sci & Eng. 2018;4:4266–77.
[112] Unger K, Salzmann P, Masciullo C, Cecchini M, Koller G, Coclite AM. Novel light-responsive biocompatible hydrogels produced by initiated chemical vapor deposition. ACS Appl Mater Interfaces. 2017;9:17408–16.
[113] Ikeda T. Photomodulation of liquid crystal orientations for photonic applications. J Mater Chem. 2003;13:2037–57.
[114] Tanaka D, Ishiguro H, Shimizu Y, Uchida K. Thermal and photoinduced liquid crystalline phase transitions with a rod–disc alternative change in the molecular shape. J Mater Chem. 2012;22:25065–71.
[115] Ge F, Zhao Y. Microstructured actuation of liquid crystal polymer networks. Adv Funct Mater. 2020;30:1901890.
[116] White TJ, Broer DJ. Programmable and adaptive mechanics with liquid crystal polymer networks and elastomers. Nat Mater. 2015;14:1087–98.
[117] Yin L, Han L, Ge F, Tong X, Zhang W, Soldera A, et al. A novel side-chain liquid crystal elastomer exhibiting anomalous reversible shape change. Angew Chem Int Ed. 2020;59:15129–34.
[118] Martella D, Nocentini S, Nuzhdin D, Parmeggiani C, Wiersma DS. Photonic microhand with autonomous action. Adv Mater. 2017;29:1704047.
[119] Prévôt ME, Ustunel S, Hegmann E. Liquid crystal elastomers – a path to biocompatible and biodegradable 3D-LCE scaffolds for tissue regeneration. Materials. 2018;11:377.
[120] Xu Z, Pan C, Yuan W. Light-enhanced hypoxia-responsive and azobenzene cleavage-triggered size-shrinkable micelles for synergistic photodynamic and chemotherapy. Biomater Sci. 2020;8:3348–58.
[121] Yeung K-W, Dong Y, Chen L, Tang C-Y, Law W-C, Tsui GC-P, et al. Printability of photo-sensitive nanocomposites using two-photon polymerization. Nanotechnol Rev. 2020;9:418–25.
[122] White EM, Yatvin J, Grubbs III JB, Bilbrey JA, Locklin J. Advances in smart materials: Stimuli-responsive hydrogel thin films. J Polym Sci Part B: Polym Phys. 2013;51:1084–99.
[123] Chu M, Shao Y, Peng J, Dai X, Li H, Wu Q, et al. Near-infrared laser light mediated cancer therapy by photothermal effect of Fe3O4 magnetic nanoparticles. Biomaterials. 2013;34:4078–88.
[124] González-Hurtado M, Marins J, Soares BG, Briones JR, Rodríguez AR, Ortiz-Islas E. Magnetic SiO_2-Fe_3O_4 nanocomposites as carriers of ibuprofen for controlled release applications. Rev Adv Mater Sci. 2018;55:12–20.
[125] Lin N, Xie R, Zou J, Qin J, Wang Y, Yuan S, et al. Surface damage mitigation of titanium and its alloys via thermal oxidation: A brief review. Rev Adv Mater Sci. 2019;58:132–46.
[126] Li J, Li X, Luo T, Wang R, Liu C, Chen S, et al. Development of a magnetic microrobot for carrying and delivering targeted cells. Sci Robot. 2018;3:eaat8829.

[127] Zarzar LD, Kim P, Kolle M, Brinker CJ, Aizenberg J, Kaehr B. Direct writing and actuation of three-dimensionally patterned hydrogel pads on micropillar supports. Angew Chem. 2011;123:9528–32.
[128] Jin D, Chen Q, Huang T-Y, Huang J, Zhang L, Duan H. Four-dimensional direct laser writing of reconfigurable compound micromachines. Mater Today. 2020;32:19–25.
[129] Bjørge IM, Salmeron-Sanchez M, Correia CR, Mano JF. Cell behavior within nanogrooved sandwich culture systems. Small. 2020;16:2001975.
[130] Kunrath MF, Dos Santos RP, de Oliveira SD, Hubler R, Sesterheim P, Teixeira ER. Osteoblastic cell behavior and early bacterial adhesion on macro-, micro- and nanostructured titanium surfaces for biomedical implant applications. Int J oral Maxillofac Implant. 2020;35:773–81.
[131] Diop-Frimpong B, Chauhan VP, Krane S, Boucher Y, Jain RK. Losartan inhibits collagen I synthesis and improves the distribution and efficacy of nanotherapeutics in tumors. Proc Natl Acad Sci USA. 2011;108:2909–14.
[132] Hidai H, Jeon H, Hwang DJ, Grigoropoulos CP. Self-standing aligned fiber scaffold fabrication by two photon photopolymerization. Biomed Microdevices. 2009;11:643–52.
[133] Jeon H, Hidai H, Hwang DJ, Grigoropoulos CP. Fabrication of arbitrary polymer patterns for cell study by two-photon polymerization process. J Biomed Mater Res, Part A. 2010;93:56–66.
[134] Thiery JP, Acloque H, Huang RY, Nieto MA. Epithelial-mesenchymal transitions in development and disease. Cell. 2009;139:871–90.
[135] Fattet L, Yang J. Molecular and cellular mechanobiology of cancer. in Molecular and Cellular Mechanobiology. New York, NY: Springer; 2016. p. 277–90.
[136] Tayalia P, Mendonca CR, Baldacchini T, Mooney DJ, Mazur E. 3D cell-migration studies using two-photon engineered polymer scaffolds. Adv Mater. 2008;20:4494–8.
[137] Klein F, Striebel T, Fischer J, Jiang Z, Franz CM, von Freymann G, et al. Elastic fully three-dimensional microstructure scaffolds for cell force measurements. Adv Mater. 2010;22:868–71.
[138] Marino A, Ciofani G, Filippeschi C, Pellegrino M, Pellegrini M, Orsini P, et al. Two-photon polymerization of sub-micrometric patterned surfaces: investigation of cell-substrate interactions and improved differentiation of neuron-like cells. ACS Appl Mater Interfaces. 2013;5:13012–21.
[139] Li R, Jin D, Pan D, Ji S, Xin C, Liu G, et al. Stimuli-responsive actuator fabricated by dynamic asymmetric femtosecond bessel beam for in situ particle and cell manipulation. ACS Nano. 2020;14:5233–42.
[140] Wu Z, Lin X, Zou X, Sun J, He Q. Biodegradable protein-based rockets for drug transportation and light-triggered release. ACS Appl Mater Interfaces. 2015;7:250–5.
[141] Dong M, Wang X, Chen XZ, Mushtaq F, Deng S, Zhu C, et al. 3D-printed soft magnetoelectric microswimmers for delivery and differentiation of neuron-like cells. Adv Funct Mater. 2020;30:1910323.
[142] Lanza R, Langer R, Vacanti JP, Atala A. Principles of tissue engineering. Cambridge, Massachusetts: Academic Press; 2020.
[143] Zueva L, Golubeva T, Korneeva E, Makarov V, Khmelinskii I, Inyushin M. Foveolar Müller cells of the pied flycatcher: Morphology and distribution of intermediate filaments regarding cell transparency. Microscopy Microanalysis. 2016;22:379–86.
[144] Thompson JR, Worthington KS, Green BJ, Mullin NK, Jiao C, Kaalberg EE, et al. Two-photon polymerized poly(caprolactone) retinal cell delivery scaffolds and their systemic and retinal biocompatibility. Acta Biomater. 2019;94:204–18.
[145] Donate R, Monzón M, Alemán-Domínguez ME, Ortega Z. Enzymatic degradation study of PLA-based composite scaffolds. Rev Adv Mater Sci. 2020;59:170–5.
[146] Timashev P, Kuznetsova D, Koroleva A, Prodanets N, Deiwick A, Piskun Y, et al. Novel biodegradable star-shaped polylactide scaffolds for bone regeneration fabricated by two-photon polymerization. Nanomedicine. 2016;11:1041–53.
[147] Hauptmann N, Lian Q, Ludolph J, Rothe H, Hildebrand G, Liefeith K. Biomimetic designer scaffolds made of D,L-lactide-ε-caprolactone polymers by 2-photon polymerization. Tissue Eng Part B Rev. 2019;25:167–86.
[148] He J, Zhang Y, Liu X, Li H, Xiong C, Zhang L. Load-bearing PTMC-beta tri-calcium phosphate and dexamethasone biphasic composite microsphere scaffolds for bone tissue engineering. Mater Lett. 2020;260:126939.
[149] Yuan P, Qiu X, Liu T, Tian R, Bai Y, Liu S, et al. Substrate-independent polymer coating with stimuli-responsive dexamethasone release for on-demand fibrosis inhibition. J Mater Chem B. 2020;8:7777–84.
[150] Paun IA, Zamfirescu M, Luculescu CR, Acasandrei AM, Mustaciosu CC, Mihailescu M, et al. Electrically responsive microreservoires for controllable delivery of dexamethasone in bone tissue engineering. Appl Surf Sci. 2017;392:321–31.
[151] Seyed Morteza N, Yasser Z, Kyong Yop R. A facile and simple approach to synthesis and characterization of methacrylated graphene oxide nanostructured polyaniline nanocomposites. Nanotechnol Rev. 2020;9:53–60.
[152] Gittard SD, Ovsianikov A, Monteiro-Riviere NA, Lusk J, Morel P, Minghetti P, et al. Fabrication of polymer microneedles using a two-photon polymerization and micromolding process. J diabetes Sci Technol. 2009;3:304–11.
[153] Kumi G, Yanez CO, Belfield KD, Fourkas JT. High-speed multiphoton absorption polymerization: fabrication of microfluidic channels with arbitrary cross-sections and high aspect ratios. Lab a Chip. 2010;10:1057–60.
[154] Xiong Z, Dong X-Z, Chen W-Q, Duan X-M. Fast solvent-driven micropump fabricated by two-photon microfabrication. Appl Phys A. 2008;93:447–52.
[155] Wang X, Qin XH, Hu C, Terzopoulou A, Chen XZ, Huang TY, et al. 3D printed enzymatically biodegradable soft helical microswimmers. Adv Funct Mater. 2018;28:1804107.
[156] Xing J, Liu L, Song X, Zhao Y, Zhang L, Dong X, et al. 3D hydrogels with high resolution fabricated by two-photon polymerization with sensitive water soluble initiators. J Mater Chem B. 2015;3:8486–91.
[157] Pearre BW, Michas C, Tsang J-M, Gardner TJ, Otchy TM. Fast micron-scale 3D printing with a resonant-scanning two-photon microscope. Addit Manuf. 2019;30:100887.
[158] Lee K-S, Kim RH, Yang D-Y, Park SH. Advances in 3D nano/microfabrication using two-photon initiated polymerization. Prog Polym Sci. 2008;33:631–81.
[159] Maibohm C, Silvestre OF, Borme J, Sinou M, Heggarty K, Nieder JB. Multi-beam two-photon polymerization for fast large area 3D periodic structure fabrication for bioapplications. Sci Rep. 2020;10:1–10.